

1 Secretomes from Bone Marrow-derived Mesenchymal Stem Cells Enhance Periodontal
2 Tissue Regeneration

3

4

5 Takamasa Kawai, D.D.S.; Wataru Katagiri, D.D.S., Ph.D.; Masashi Osugi, D.D.S.,
6 Ph.D.; Yukiko Sugimura, D.D.S.; Hideharu Hibi, D.D.S., Ph.D.; Minoru Ueda, D.D.S.,
7 Ph.D

8

9

10 Department of Oral and Maxillofacial Surgery, Nagoya University Graduate School of
11 Medicine, Nagoya, Japan

12

13 Corresponding author: Wataru Katagiri D.D.S., Ph.D

14 Department of Oral and Maxillofacial Surgery, Nagoya University Graduate

15 School of Medicine

16 65 Tsurumai-cho, Showa-ku, Nagoya, Aichi 466-8550, Japan

17 Tel +81-52-744-2348 Fax +81-52-744-2352

18 E-mail: w-kat@med.nagoya-u.ac.jp

19

20

21

22

23

24

25 **Abstract**

26

27 *Background aims.* Periodontal tissue regeneration using mesenchymal stem cells
28 (MSCs) has been regarded as a future cell-based therapy. However, low survival rates
29 and the potential tumorigenicity of implanted MSCs could undermine the efficacy of
30 cell-based therapy. The use of conditioned media from MSCs (MSC-CM) may be a
31 feasible approach to overcome these limitations. The aim of this study is to confirm the
32 effect of MSC-CM on periodontal regeneration.

33 *Methods.* MSC-CM were collected during their cultivation. The concentrations of the
34 growth factors in MSC-CM were measured using ELISA. Rat MSCs (rMSCs) and
35 human umbilical vein endothelial cells (HUVEC) cultured in MSC-CM were assessed
36 on wound healing and angiogenesis. The expressions of osteogenetic and
37 angiogenic-related genes of rMSCs cultured in MSC-CM were quantified by real-time
38 RT-PCR analysis. *In vivo*, periodontal defects were prepared in the rat models and the
39 collagen sponges with MSC-CM were implanted.

40 *Results.* MSC-CM includes IGF-1, VEGF, TGF- β 1 and HGF. *In vitro*, wound healing
41 and angiogenesis increased significantly in MSC-CM. The levels of expression of
42 osteogenetic and angiogenic-related genes were significantly upregulated in rMSCs
43 cultured with MSC-CM. *In vivo*, in the MSC-CM group 2 weeks after implantation,
44 immunohistochemical analysis showed several CD31-, CD105-, or FLK-1-positive cells
45 occurring frequently. At 4 weeks after implantation, a regenerated periodontal tissue
46 was observed in MSC-CM groups.

47 *Conclusions.* The use of MSC-CM may be an alternative therapy for periodontal tissue
48 regeneration because several cytokines included in MSC-CM will contribute to many

49 processes of complicated periodontal tissue regeneration.

50

51 **Key Words:** *periodontal regeneration, mesenchymal stem cell, conditioned medium,*

52 *paracrine effects, angiogenesis, migration*

53

54

55

56

57

58

59

60

61

62

63

64

65

66

67

68

69

70

71

72

73 **Abbreviations**

74 mesenchymal stem cells (MSCs), human MSCs (hMSCs), platelet-rich plasma (PRP),
75 conditioned media (CM), human bone marrow-derived MSCs (MSC-CM), insulin-like
76 growth factor-1 (IGF-1), vascular endothelial growth factor (VEGF), transforming
77 growth factor- β 1 (TGF- β 1), hepatocyte growth factor (HGF), fibroblast growth factor
78 (FGF)-2, platelet-derived growth factor (PDGF)-BB, bone morphogenetic protein
79 (BMP)-2, stromal-cell-derived factor (SDF)-1, rat periodontal ligament cells (rPDLs),
80 fetal bovine serum (FBS), Dulbecco's Modified Eagle Medium (DMEM),
81 enzyme-linked immunosorbent assay (ELISA), Rat MSCs (rMSCs), human umbilical
82 vein endothelial cells (HUVEC), human diploid fibroblasts (HDF), optimized
83 angiogenesis medium (BM), DMEM-10% FBS (EM; Expansion Medium), *Alkaline*
84 *phosphatase (ALP)*, *Osteocalcin (OCN)*, *angiopoietin 1 (ANG-1)*, *angiopoietin 2*
85 *(ANG-2)*, atelo-collagen sponge (ACS)

86

87 **Introduction**

88

89 The chronic presence of plaque bacteria in the gingival and periodontal tissues results in
90 destruction of structural components of the periodontium (1). This condition leads to the
91 clinical signs of periodontitis, with the breakdown of periodontal tissue, resulting in
92 tooth loosening (2). To regenerate lost periodontal tissue, numerous procedures and
93 products have been developed, for example, autogenous bone grafting (3), guided tissue
94 regeneration (GTR) (4), platelet-rich plasma (5), enamel matrix derivatives
95 (Emdogain[®]) (6), and recombinant human growth factors (7-12). Although these
96 treatments have been reported to be effective in regenerating periodontal tissue,
97 candidates for such treatments are limited, and the amount of tissue that is regenerated
98 cannot be reliably predicted.

99 Cell therapy with stem cells is a promising approach for treating various refractory
100 diseases. Therefore, periodontal tissue regeneration using mesenchymal stem cells
101 (MSCs) has been regarded as a viable future cell-based therapy for the treatment of
102 periodontal diseases (13, 14).

103 We previously used a mixture of human MSCs (hMSCs) and platelet-rich plasma (PRP)
104 (hMSCs/PRP) as bone graft materials, with predictable outcomes (15). However, recent
105 studies of MSC transplantation in an acute myocardial infarction revealed that the
106 implanted MSCs did not survive, and only 4.4% of engraftment of MSCs could be
107 found 1 week after transplantation (16). The studies of MSC transplantation in cases of
108 spinal cord injury revealed that the implanted MSCs disappeared from the host tissue
109 1–2 weeks after transplantation (17). These facts suggest that the implanted cells may
110 contribute to tissue regeneration through them as well as their paracrine effects. Many

111 secretomes, including growth factors and cytokines, have been reported in the
112 conditioned media (CM) of various MSCs (18-20), which could be responsible for the
113 paracrine effects of stem cells on tissue regeneration. Previous studies have reported the
114 use of CM for experimental regenerative therapies. For example, CM obtained from
115 amniotic fluid-derived MSCs (21) and adipose-derived stem cells (21) significantly
116 enhanced wound healing. Endothelial progenitor cell CM induced neovascularization in
117 a rat hindlimb ischemia model (22).

118 The use of CM has the added benefit of solving several problems currently encountered
119 in clinical applications of stem cells, such as tumorigenesis (23) and the transmission of
120 infectious diseases.

121 We previously reported that CM transplantation from human bone marrow-derived
122 MSCs (MSC-CM) promoted bone regeneration in a rat calvarial bone defect model.
123 MSC-CM contributed to accelerated mobilization of endogenous MSCs and endothelial
124 cells for bone regeneration (24, 25). These effects of MSC-CM transplantation were
125 stronger than those of MSC implantation. MSC-CM has plural growth factors and
126 cytokines related to tissue regeneration, such as insulin-like growth factor-1 (IGF-1),
127 vascular endothelial growth factor (VEGF), transforming growth factor- β 1 (TGF- β 1),
128 and hepatocyte growth factor (HGF).

129 Based on these findings, we hypothesized that the cytokines contained in MSC-CM may
130 enhance mobilization of endogenous MSCs and angiogenesis and promote periodontal
131 tissue regeneration through several steps. At the cellular level, the process of
132 periodontal tissue regeneration requires angiogenesis, cell migration, and proliferation
133 and differentiation into various cell types, particularly osteoblasts and cementoblasts,
134 and the cytokines contained in MSC-CM can contribute these biological steps toward

135 osteogenesis.

136 Angiogenesis is especially crucial to the accelerated regeneration of lost tissues in
137 periodontal therapy because the process of periodontal tissue regeneration is
138 complicated, as periodontal wound healing occurs on the nonvascular and nonvital hard
139 tissues of the root surface (26).

140 The purpose of this study was to confirm the effect of MSC-CM and its role in
141 periodontal regeneration.

142 **Materials and Methods**

143

144 *Ethics Statement*

145 All animal protocols were approved by the Animal Care and Use Committee of Nagoya
146 University Graduate School of Medicine (Approval ID number: 25375). Maximum
147 efforts were made to minimize suffering, and all surgery and measurement under
148 inserting catheter were performed under deep anesthesia.

149

150 *Cell preparation*

151 Human MSCs (hMSCs) were purchased from Lonza Inc. (Walkersville, MD, USA) and
152 cultured in mesenchymal stem cell basal medium (MSCBM; Lonza Inc.) containing
153 MSCGM SingleQuots (Lonza Inc.) at 37 °C in 5% CO₂/95% air. After primary culture,
154 the cells were subcultured at a density of approximately 1×10^4 cells/cm². hMSCs at the
155 3rd to the 9th passages were used for experiments. Subconfluent hMSCs were
156 trypsinized and used for cell implantation.

157 Rat MSCs (rMSCs) was isolated from 7-week-old Wistar/ST rats weighing 180–210 g
158 (Japan SLC, Shizuoka, Japan) as previously reported (27). Briefly, donor rats were
159 sacrificed and the femora were dissected out. Using sterile conditions, the edge of each
160 bone was cut, Dulbecco's modified Eagle's medium (DMEM; Gibco, Rockville, MD)
161 was injected into the bone marrow using a 25-gauge syringe, the bone marrow cells
162 were flushed out to the opposite side, and this maneuver was repeated several times.
163 The marrow was then seeded into each tissue culture flask in DMEM containing
164 antibiotic-antimycotic (100 units/mL penicillin G, 100 mg/mL streptomycin, and 0.25
165 mg/mL amphotericin B; Gibco) and the medium was supplemented with 10% fetal

166 bovine serum (FBS). Three days after seeding, floating cells were removed and the
167 medium was replaced with fresh medium. The adherent, spindle-shaped cells were
168 passaged when the cells were approaching confluence. Adherent cells were collected
169 using trypsin/EDTA, resuspended in fresh medium, and transferred to new flasks at a
170 density of 1×10^4 cells/cm². rMSCs obtained from cultures at the 2nd to the 4th
171 passages were used for the experiments.

172 Rat periodontal ligament cells (rPDLCs) were isolated from the periodontal ligament
173 tissue of 7-week-old Wistar/ST rats. Periodontal ligament was gently removed from the
174 middle third of the mandibular molar root surface and digested in an equal volumes of
175 Type I collagenase (3 mg/mL) and Type II dispase (4 mg/mL) for 1 h at 37°C. The
176 resulting cells (1×10^4 cells/cm²) were then seeded into each tissue culture flask in α
177 -MEM culture medium (Sigma-Aldrich Inc., St Louis, MO, USA) supplemented with
178 10%FBS, 100 μ M L-ascorbate-2-phosphate (Sigma-Aldrich, St. Louis, MO, USA),
179 2mM L-glutamine and antibiotic-antimycotic (100 units/mL penicillin G, 100 mg/mL
180 streptomycin, and 0.25 mg/mL amphotericin B; Gibco). Single cell colonies were
181 observed and passage (P0) cells were cultured. rPDLCs obtained from cultures at the
182 3rd to the 5th passages were used for the experiments.

183 Pluripotency of obtained cells for differentiation into classical mesenchymal lineage
184 cells, including osteoblasts, adipocytes, or chondrocytes, was verified by using
185 previously reported methods. These cells were used as rMSCs in this study (data not
186 shown). The results indicated that these cells had stem cell characteristics.

187

188 *Preparation of conditioned media (CM)*

189 hMSCs that were 70%–80% confluent were re-fed with serum-free medium. The
190 cell-cultured CM were collected after a 48-h incubation. Collected cultured CM were
191 defined as hMSC-cultured CM (MSC-CM) and were stored at 4 or –80 °C before using
192 for the following experiments.

193

194 *Enzyme-linked immunosorbent assay (ELISA)*

195 The levels of IGF-1, VEGF, TGF- β 1, HGF, fibroblast growth factor (FGF)-2,
196 platelet-derived growth factor (PDGF)-BB, bone morphogenetic protein (BMP)-2, and
197 stromal-cell-derived factor (SDF)-1 in MSC-CM were investigated using
198 enzyme-linked immunosorbent assay (ELISA). The concentration of these factors was
199 measured using a Human Quantikine ELISA kit (R&D Systems, Minneapolis, MN)
200 according to the manufacturer's instructions. Briefly, 200 μ L of MSC-CM,
201 DMEM-0%FBS, or DMEM-30%FBS was added to 96-well microplates that were
202 coated with a monoclonal antibody to the factor of interest and incubated for 2 h. After
203 washing with PBS, a horseradish peroxidase-conjugated cytokine or
204 growth-factor-specific antibody was added to each well, incubated for 2 h, and washed.
205 Substrate solution was added and incubated for 30 min, and the reaction was terminated
206 by addition of the stop solution. Cytokine/growth factor levels were determined by
207 measurement of the optical density at 450nm using a microplate spectrophotometer
208 (Benchmark Plus; Bio-Rad, Hercules, CA).

209

210

211 *Wound-healing assay*

212 The migratory properties of rMSCs and rPDLCs were examined using the CytoSelect

213 Wound Healing Assay kit (Cell Biolabs, San Diego, CA, USA) according to the
214 manufacturer's instructions. Briefly, cell suspension was added to the well with a plastic
215 insert in place. The insert was removed from the well after a monolayer of cells had
216 formed, creating a wound gap of 0.9 mm. After washing, cells were incubated at 37 °C
217 for 48 h in MSC-CM with 30% FBS or serum-free DMEM. The extent of wound
218 closure was determined with a light microscope (CK40; Olympus, Tokyo, Japan).

219

220 *Tube formation assay*

221 An angiogenesis assay kit (KZ-1000; Kurabo, Osaka, Japan) was used according to the
222 manufacturer's instructions (28). This kit comprised a 24-well culture dish in which
223 human umbilical vein endothelial cells (HUVECs) and human diploid fibroblasts (HDF)
224 were seeded in the optimal condition for capillary tube formation. The optimized
225 angiogenesis medium (BM) in each well was changed on days 1, 4, 7, and 9 with fresh
226 medium containing VEGF (10 ng/mL), MSC-CM, MSC-CM plus anti-VEGF
227 (MAB293) (10 µg/mL) (R&D Systems), or none. The antibody concentration was 10
228 µg/mL and therefore was 100-fold greater than that for half-maximal inhibition of 10
229 ng/mL of the recombinant proteins.

230 After 11 days, cells were fixed in 70% ethanol and incubated with diluted primary
231 antibody (mouse anti-human CD31, 1:4000) for 1 h at 37 °C, and with the secondary
232 antibody (goat anti-mouse IgG alkaline-phosphatase-conjugated antibody, 1:500) for 1
233 h at 37 °C, with visualization achieved using 5-bromo-4-chloro-3-indolyl
234 phosphate/nitro blue tetrazolium. Images were obtained from five different fields (5.5
235 mm²/field) for each well, and tube length (the total lengths of the tubes) and joints (the
236 number of capillary connections) were quantified using Angiogenesis Image Analyzer

237 Ver.2 (Kurabo).

238

239 *Real-time RT-PCR*

240 rMSCs were cultured with MSC-CM or DMEM-10% FBS (EM; Expansion Medium)
241 for 48 h, and total RNA was extracted using an RNeasy Mini kit (QIAGEN GmbH,
242 Hilden, Germany) according to the manufacturer's protocol. Real-time RT-PCR
243 analysis was performed as previously described (29). Samples for total RNA
244 determination (50 ng each) were placed into a 50- μ L-volume RT-PCR tube. The
245 sequences of the specific primers and probes used for the real-time RT-PCR analysis for
246 *Alkaline phosphatase (ALP)*, *Osteocalcin (OCN)*, *Runx2*, *VEGF-A*, *angiopoietin 1*
247 (*ANG-1*), *angiopoietin 2 (ANG-2)*, and *GAPDH* are given in Table 1. RT-PCR reactions
248 and the resulting relative increase in reporter fluorescent dye emission were monitored
249 in real time using the 7000 sequence detector (Perkin-Elmer, Foster City, CA, USA).
250 Signals were analyzed using a sequence detector 1.0 program (Perkin-Elmer). The PCR
251 conditions were as follows: 1 cycle at 50 °C for 2 min, 1 cycle at 60 °C for 30 min, 1
252 cycle at 95 °C for 5 min, 50 cycles at 95 °C for 20 s, and then 60 °C for 1 min. The
253 relative amount of each mRNA in one sample was obtained by calculation of the
254 respective standard curves. The standard curves for each mRNA were drawn using
255 different concentrations (2000, 400, 80, 16, and 3.2 ng) of the total RNA of rMSCs. The
256 relative expression levels were normalized to GAPDH expression.

257

258 *Rat periodontal defect model*

259 Adult male Wistar/ST rats were purchased from Japan SLC (Shizuoka, Japan). The rats
260 were housed on a 12 hours light/dark cycle in a temperature-and-humidity-controlled

261 room with food and water ad libitum. The animals were allowed to acclimatize for at
262 least seven days before the start of the experiments. Surgery was performed in a similar
263 fashion as previously described (14) using magnification loupes. Ten-week-old male
264 Wistar/ST rats weighing 260–290 g were anesthetized by intraperitoneal injection of
265 Somnopentyl[®] (20 mg/kg body weight). With the rat in the supine position, a mucosal
266 incision was made from the gingival sulcus of the second molar mesial palatal side to
267 the first molar mesial palatal side, and an approximately 5-mm incision was made
268 continuously in the mesial direction from the first molar mesial side. After mucosal flap
269 elevation, the periodontal tissue, including the cementum, alveolar bone, and
270 periodontal ligament, was bilaterally excised at the palatal side of the first molar using a
271 dental round bur (ISO standard 010) under irrigation, so that the dimensions of the
272 defect were approximately 1 mm in diameter. After irrigation with physiological saline
273 solution, the experimental materials were then implanted into the defects. An absorbable
274 atelo-collagen sponge (ACS) (TERUDERMIS[®]; Olympus Terumo Biomaterials, Tokyo,
275 Japan) was used as a scaffold and contained 30 μ L MSC-CM or PBS. The rats with
276 defects were implanted with graft materials: MSC-CM with ACS (MSC-CM group),
277 PBS with ASC (PBS group), or defect only (Defect group). Finally, the mucosal flaps
278 were replaced using 6-0 polydioxanone sutures (PDS II; Ethicon Inc., Somerville, N.J.,
279 USA). During the surgery, the body temperature was maintained at 37°C using a
280 homeothermic heating pad. Following the surgery, the rats were administered
281 buprenorphine (0.05 mg/kg, i.m. per 12 hours) for 24 hours to relieve pain. The rats
282 were were euthanized by an overdose of ether (Wako, Osaka, Japan) on 2 or 4 weeks
283 after transplantation (n = 8 at each time point in each group).

284

285 *Histological analyses*

286 Explants were decalcified with K-CX solution (Falma Co., Tokyo, Japan), and were
287 then dehydrated using graded ethanol, cleared with xylene, and embedded in paraffin.
288 The specimens were cut in a sagittal direction to make 5- μ m-thick histological sections
289 in the buccal–palatal plane and were stained with hematoxylin and eosin. Histological
290 analysis was performed using a light microscope (CK40; Olympus, Tokyo, Japan).

291

292 *Immunohistochemical staining*

293 MSC-CM or PBS with ACS was implanted into rat periodontal defects, and samples
294 were collected after 2 weeks. Fresh-frozen sections of these samples were made
295 according to the Kawamoto method using a Multi-Purpose Cryosection Preparation Kit
296 (30). Cryofilm type 2C was applied to the cutting surface of the completely frozen block,
297 which was cut with a tungsten carbide knife at -25°C in a cryostat chamber (Leica
298 CM3050S; Leica Microsystems, Wetzlar, Germany). The section was fixed with 100%
299 ethanol for 10 min and then washed with PBS for 3 min. CD31, a monoclonal mouse
300 antibody (BD Pharmingen), was used as a marker for rat endothelial cells. CD105, a
301 polyclonal rabbit antibody (Santa Cruz Biotechnology, Inc., Santa Cruz, CA, USA), was
302 used as a marker for rat stem cells. Flk-1, a monoclonal mouse antibody (Santa Cruz
303 Biotechnology), was used as a marker for VEGF-R2. An Alexa Fluor 633-conjugated
304 goat anti-mouse IgG (Molecular Probes, Inc., Eugene, OR, USA) and an Alexa Fluor
305 488-conjugated donkey anti-rabbit IgG (Molecular Probes, Inc.) were used as secondary
306 antibodies. After DAPI staining, the section was washed with PBS and mounted
307 between a glass slide and the adhesive film. The section was enclosed by the mounting
308 resin SCMM R2 on the glass slide, and the resin was hardened with UV irradiation for 1

309 min by means of the UV Quick Cryosection Mounter (ATTO Bio-Instrument, Tokyo,
310 Japan). After fixation, the specimen was observed by a fluorescence microscope
311 (BZ9000; Keyence Co., Osaka, Japan).

312

313 *Statistical analysis*

314 All values are expressed as the mean \pm SD. Comparisons of results between
315 experimental groups and control groups were analyzed with Tukey's HSD (Honestly
316 Significant Difference) test. Statistical analyses were performed using the SPSS version
317 22.0.0 software package. If the *P* -value was <0.05 , the result obtained was considered
318 to be significant.

319

320 **Results**

321

322 *Growth factors included in MSC-CM*

323 In MSC-CM, the concentrations of IGF-1, VEGF, TGF- β 1, and HGF were $1515.6 \pm$
324 211.8 pg/mL, 465.8 ± 108.8 pg/mL, 339.8 ± 14.4 pg/mL, and 20.3 ± 7.9 pg/mL,
325 respectively. No other factors were detected in MSC-CM, DMEM (-), or 30% FBS
326 (Table 2).

327

328

329 *Effects of MSC-CM on rMSC and rPDLC migration and proliferation*

330 The percentage of rMSCs in the wound area of DMEM (-) was $9.28 \pm 4.41\%$. There
331 were $70.9 \pm 6.8\%$ rMSCs in the wound area of positive control (30% FBS). MSC-CM
332 exerted significant effects ($p < 0.01$) and closed the wound to $43.4 \pm 10.6\%$ rMSCs

333 (Figure 1).

334 The percentage of rPDLCs in the wound area of DMEM (-) was $2.36 \pm 2.32\%$, with
335 $48.01 \pm 6.28\%$ in 30% FBS and $17.98 \pm 4.14\%$ in MSC-CM. Thus, MSC-CM increased
336 rMSC migration more than four-fold and rPDLC migration more than seven-fold
337 compared with that in DMEM (-). These differences were statistically significant ($p <$
338 0.01), indicating that MSC-CM enhanced rMSC and rPDLC migration and proliferation
339 (Figure 1).

340

341

342 *Effects of MSC-CM on tube formation of HUVECs*

343 In the presence of BM and BM with anti-VEGF, HUVECs did not demonstrate tube
344 formation. In contrast, BM with MSC-CM or VEGF stimulated tube formation (Figure
345 2A). The tube lengths were 18341.59 ± 3453.14 pixels, 20987.50 ± 2053.97 pixels,
346 11244.35 ± 1662.13 pixels, and 11542.33 ± 1869.95 pixels in BM with MSC-CM, in
347 BM with VEGF, in BM with MSC-CM and anti-VEGF, and in BM only, respectively
348 (Figure 2B). The number of joints were 72.36 ± 20.72 , 81.81 ± 15.86 , 42.66 ± 15.27 ,
349 and 38.06 ± 12.42 , respectively (Figure 2C). The tube lengths and the number of joints
350 were significantly greater in BM with MSC-CM than in BM with MSC-CM plus
351 anti-VEGF and in BM only.

352

353

354 *MSC-CM enhanced osteogenic and angiogenic marker gene expression*

355 The levels of expression of the *ALP*, *OCN*, *Runx2*, *VEGF-A*, *ANG-1*, and *ANG-2* genes
356 were significantly upregulated in rMSCs cultured with MSC-CM compared with rMSCs

357 cultured in EM (Figure 3).

358

359

360 *MSC-CM induced periodontal tissue regeneration*

361 Two weeks after MSC-CM implantation into the periodontal tissue defect, a small
362 amount of bone regeneration from the residual bone was evident, and a cell mass had
363 accumulated adjacent to the regenerated bone (Figure 4A, 4B). In contrast, the PBS and
364 Defect groups did not show bone or periodontal tissue regeneration (Figure 4C–4F). In
365 addition, particularly in the Defect group, inflammatory cell infiltration was seen in the
366 periodontal defect site.

367 Four weeks after MSC-CM implantation into the periodontal tissue defect, the
368 regenerated bone and other periodontal tissues were observed in the defect (Figure 5A,
369 5B). A cementum-like structure was noted on the superficial surface of the dentin, and
370 the regenerated bone exhibited alveolar crista. Moreover, a periodontal-ligament-like
371 structure was seen between the cementum and the regenerated bone. In contrast, the
372 PBS and Defect groups did not have any periodontal tissue, except for regeneration of a
373 small amount of the alveolar bone (Figure 5C–5F).

374

375

376 *Immunohistochemical analysis for CD31, CD105, and FLK-1 expression in periodontal*
377 *tissue defects*

378 In the MSC-CM group, numerous CD31-, CD105-, or FLK-1-positive cells occurred
379 particularly frequently on the periphery of PDL, surface of the alveolar bone, and dental
380 root. In contrast, there were fewer CD31-, CD105-, or FLK-1-positive cells in both the

381 PBS and Defect groups (Figure 6).

382 **Discussion**

383

384 The results from this study suggested that several cytokines and chemokines present in
385 MSC-CM promote periodontal tissue regeneration through various processes, such as
386 mobilization of endogenous MSCs, angiogenesis, and differentiation.

387 Recently, attempts have begun to establish treatments to accelerate periodontal tissue
388 regeneration by local application of human recombinant cytokines to stimulate
389 proliferation and differentiation into hard tissue-forming cells, such as cementoblasts
390 and osteoblasts (31) from endogenous MSCs, as well as promote periodontal tissue
391 regeneration. Direct local application of combination of factors, such as PDGF and
392 IGF-I (7), BMP-2 (8), TGF- β (9), osteogenic protein (OP)-1 (10), and brain-derived
393 neurotrophic factor (BDNF) (11), stimulates and promotes regional periodontal tissue
394 regeneration *in vivo*. In addition, the clinical trials of FGF-2 and PDGF-BB for
395 periodontal tissue regeneration in human have been reported (12). However, application
396 of a single growth factor has limited tissue regeneration ability, and the amount of tissue
397 that is regenerated cannot be predicted (32). In addition, application of a single growth
398 factor such as BMP-2 requires superphysiological doses (33) and may induce a severe
399 inflammatory response (34). Therefore, a combination of several different factors will
400 likely be better for optimizing bone regeneration (35).

401 The present results of the wound-healing assay show that MSC-CM enhanced migration
402 and proliferation of rMSCs and rPDLs. In addition, to confirm that endogenous MSCs
403 migrated to the site where MSC-CM was implanted, we performed
404 immunohistochemical staining of the periodontal defects of rats with anti-CD105
405 antibodies after a 2-week implantation. A large number of CD105-positive cells,

406 reported to be specific markers of MSCs (36), existed in periodontal defects compared
407 with the PBS and Defect groups. These results indicate that MSC-CM has the potential
408 to mobilize endogenous MSCs and to promote periodontal tissue regeneration. In our
409 previous study (24), the injected MSCs from the rat caudal vein migrated into the
410 calvarial bone defect where MSC-CM was implanted. Similarly, in the results of
411 immunohistochemical analysis for CD44 expression as markers of MSCs (36) in the
412 bone defects of rats, numerous CD44-positive cells and tubular formations were
413 detected in the calvarial bone defects of the MSC-CM group compared with the PBS
414 and Defect groups, indicating that the migration of endogenous MSCs and angiogenesis
415 were induced by MSC-CM (24). IGF-1 induces osteoblast proliferation and migration
416 (37, 38) and enhances periodontal regeneration by stimulating PDL cells through the
417 PI3K pathway (39).

418 The results of real-time RT-PCR in this study and the levels of expression of osteogenic
419 marker genes, *ALP*, *OCN*, and *Runx2*, were significantly upregulated in rMSCs cultured
420 with MSC-CM compared with rMSCs cultured in EM. This indicates that MSC-CM
421 promotes osteoblastic differentiation of rMSCs. From histological findings of this study,
422 MSC-CM had dramatic effects on periodontal tissue regeneration. In the MSC-CM
423 groups after a 2-week implantation, bone regeneration from the residual bone was
424 evident, but the other groups showed no bone regeneration. Four weeks after MSC-CM
425 implantation, the regenerated bone exhibited alveolar crista. From these finding, it was
426 obvious that MSC-CM promoted stem cell differentiation into the osteoblastic lineage
427 after endogenous cell mobilization and bone regeneration in the periodontal tissue
428 defect had occurred.

429 VEGF is the main regulator of angiogenesis as well as contributes to osteogenesis (40).

430 TGF- β 1 increases bone formation by recruiting osteoprogenitor cells and stimulating
431 their proliferation and differentiation into osteocytes (41).

432 Compared with the results from a previous study using the same rat model with MSC
433 implantation, the histological results from this study at 4 weeks after implantation were
434 equivalent to those from the other study at 8 weeks after implantation (14). In the
435 MSC-CM groups, a regenerated bone and other periodontal tissues such as a
436 cementum-like structure and a periodontal-ligament-like structure were observed after a
437 4-week implantation. Conversely, these were observed after a 4-week MSC
438 implantation.

439 To regenerate periodontal tissue destroyed by periodontitis, several events including
440 angiogenesis, cell migration, and proliferation and differentiation of various cell types,
441 particularly osteoblasts and cementoblasts will be required. This process is complicated
442 by the fact that periodontal wound healing occurs on the nonvascular and nonvital hard
443 tissues of the root surface. Thus, periodontal tissue regeneration critically relies on the
444 re-establishment and proper function of the damaged vascular system.

445 In the present study, to confirm the effects of MSC-CM on angiogenesis *in vitro*, we
446 performed the tube formation assay, which showed that MSC-CM strongly promotes
447 angiogenesis. From the results of the real-time RT-PCR in this study, the levels of
448 expression of angiogenic marker genes, *VEGF-A*, *ANG-1*, and *ANG-2*, were
449 significantly upregulated in rMSCs cultured with MSC-CM compared with rMSCs
450 cultured in EM. *ANG1* causes chemotaxis of endothelial cells and stimulates
451 angiogenesis (42-43). *ANG2* also stimulates angiogenesis in the presence of VEGF (44).

452 *In vivo*, in the MSC-CM groups after a 2-week implantation, immunohistochemical
453 staining showed that many CD31- and FLK-1-positive cells existed in periodontal

454 defects compared with the PBS and Defect groups. The results that MSC-CM with
455 anti-VEGF antibody did not promote tube formation of HUVECs and that more
456 FLK-1-positive cells existed in the MSC-CM groups than in other groups in the
457 immunohistochemical analysis indicate that VEGF exerts the effects of MSC-CM
458 primarily on angiogenesis. VEGF is well known to enhance angiogenesis in tissue
459 regeneration by promoting proliferation and migration of vascular endothelial cells (45).
460 Other factors known to relate to angiogenesis, such as HGF and TGF- β 1, were also
461 detected in MSC-CM in the present study. HGF reportedly potentiates the angiogenic
462 effect of VEGF by inducing its upregulation (46, 47). TGF- β 1 plays an important role in
463 the process whereby pericytes exert a stabilizing effect on newly formed vessels (43).
464 Several recent studies have suggested that perhaps almost all MSCs are normally
465 resident as pericytes before isolation and that MSCs express aspects of the pericyte
466 phenotype (48, 49). In other reports, MSCs have also been shown to differentiate into
467 SMA⁺ pericytes after implantation into a hind-leg ischemia model (50). It is presumed,
468 because of the results of the wound-healing assay in this study, that MSC-CM enhances
469 the migration and proliferation of pericytes and contributes to angiogenesis. Thus, we
470 predict that MSC-CM directly promotes angiogenesis by some cytokines as well as
471 indirectly mediates endogenous MSCs, including pericytes, to participate in
472 angiogenesis.

473 From the results of real-time RT-PCR in this study, the levels of expression of
474 osteogenic marker genes, *ALP*, *OCN*, and *Runx2*, were significantly upregulated in
475 rMSCs cultured with MSC-CM compared with rMSCs cultured in EM, indicating that
476 MSC-CM promoted the osteoblastic differentiation of rMSCs.

477 The human PDL contains a subpopulation of stem cells that are responsible for

478 maintaining and regenerating periodontal tissue structure and function (31). These cells
479 exhibit multipotency, as demonstrated by their ability to differentiate into osteoblasts,
480 fibroblasts, and cementoblasts and form cementum- and PDL-like tissues. In addition,
481 progenitor cells responsible for alveolar bone formation lie in PDL or around the blood
482 vessels. From the present results of immunohistochemical analysis in periodontal tissue
483 defects after a 2-week implantation, in the MSC-CM group, numerous CD31-, CD105-,
484 or FLK-1-positive cells occurred particularly frequently on the periphery of PDL,
485 surface of the alveolar bone, and dental root. These results indicated that MSC-CM
486 effectively promoted periodontal tissue regeneration because it contributed to the
487 angiogenesis, mobilization, and differentiation into cementoblasts and osteoblasts of
488 endogenous MSCs, leading to the regenerated alveolar bone, cementum tissue, and
489 PDL.

490 From the results of this study, it was suggested that MSC-CM contributes to
491 upregulation of several processes of periodontal tissue regeneration through the
492 angiogenesis and mobilization of endogenous MSCs, and thus enhanced periodontal
493 regeneration. Using MSC-CM for periodontal tissue regeneration may be effective
494 because several cytokines, including MSC-CM, contribute several processes to the
495 complex system of periodontal tissue regeneration.

496 In this study, we also used hMSCs and their cultured conditioned media for periodontal
497 tissue regeneration because our aim was to apply MSC-CM to human patients and we
498 investigated MSC-CM for drug discovery as a preclinical trial. We previously reported
499 that MSC-CM promoted bone regeneration in a rat calvarial bone defect model (24, 25).
500 In these studies, it was suggested that MSC-CM suppress T-lymphocyte proliferation
501 and MSC-CM is useful for xenogeneic transplantation (24). Additionally, there was less

502 infiltration of inflammatory cells in the MSC-CM group compared with the other group
503 without immunosuppressive drug in histological analysis (25). As a result,
504 transplantation of MSC-CM to rats didn't enhance the immune response but contributed
505 periodontal tissue regeneration in this study. If MSC-CM treatment protocol is to be
506 established for periodontal regeneration, it is essential that effective and therapeutic
507 doses of MSC-CM as well as the safety of the therapy should be carefully established.
508 Further investigation regarding these matters including transplantation to large animals
509 is now in progress.

510

511 **Acknowledgments**

512

513 The authors thank the members of the Department of Oral and Maxillofacial Surgery of
514 Nagoya University Graduate School of Medicine for their help and contributions to the
515 completion of this study.

516

517 ***Declaration of interest:***

518 The authors report no conflicts of interest. The authors alone are responsible for the
519 content and writing of the paper.

520

521 **References**

522

- 523 1. Pihlstrom BL, Michalowicz BS, Johnson NW. Periodontal diseases. *Lancet*.
524 2005;366:1809-20.
- 525 2. Kikuchi T, Mitani A, Noguchi T. The mechanism of bone resorption in chronic
526 inflammation of periodontal disease. *Clin Calcium*. 2006;16:241-47.
- 527 3. Gantes B, Martin M, Garrett S, Egelberg. Treatment of periodontal furcation defects.
528 (II). Bone regeneration in mandibular class II defects. *J Clin Periodontol*.
529 1988;15:232-9.
- 530 4. Villar CC, Cochran DL. Regeneration of periodontal tissues: guided tissue
531 regeneration. *Dent Clin North Am*. 2010;54:73-92.
- 532 5. Anitua E, Troya M, Orive G. An autologous platelet-rich plasma stimulates
533 periodontal ligament regeneration. *J Periodontol*. 2013;84:1556-66.
- 534 6. Esposito M, Grusovin MG, Papanikolaou N, Coulthard P, Worthington HV. Enamel
535 matrix derivative (Emdogain (R)) for periodontal tissue regeneration in intrabony
536 defects. *Cochrane Database Syst Rev*. 2009:69.
- 537 7. Lynch SE, Williams RC, Polson AM, Howell TH, Reddy MS, Zappa UE, et al. A
538 combination of platelet-derived and insulin-like growth factors enhances periodontal
539 regeneration. *J Clin Periodontol*. 1989;16:545-8.
- 540 8. Kinoshita A, Oda S, Takahashi K, Yokota S, Ishikawa I. Periodontal regeneration
541 by application of recombinant human bone morphogenetic protein-2 to horizontal
542 circumferential defects created by experimental periodontitis in beagle dogs. *J*
543 *Periodontol*. 1997;68:103-9.
- 544 9. Mohammed S, Pack ARC, Kardos TB. The effect of transforming growth factor

- 545 beta one (TGF-beta(1)) on wound healing, with or without barrier membranes, in a
546 Class II furcation defect in sheep. *J Periodontal Res.* 1998;33:335-44.
- 547 10. Giannobile WV, Ryan S, Shih MS, Su DL, Kaplan PL, Chan TCK. Recombinant
548 human osteogenic protein-1 (OP-1) stimulates periodontal wound healing in class
549 III furcation defects. *J Periodontol.* 1998;69:129-37.
- 550 11. Takeda K, Shiba H, Mizuno N, Hasegawa N, Mouri Y, Hirachi A, et al.
551 Brain-derived neurotrophic factor enhances periodontal tissue regeneration. *Tissue*
552 *Eng.* 2005;11:1618-29.
- 553 12. Nevins M, Giannobile WV, McGuire MK, Kao RT, Mellonig JT, Hinrichs JE, et al.
554 Platelet-derived growth factor stimulates bone fill and rate of attachment level gain:
555 Results of a large multicenter randomized controlled trial. *J Periodontol.*
556 2005;76:2205-15.
- 557 13. Tsumanuma Y, Iwata T, Washio K, Yoshida T, Yamada A, Takagi R, et al.
558 Comparison of different tissue-derived stem cell sheets for periodontal regeneration
559 in a canine 1-wall defect model. *Biomaterials.* 2011;32:5819-25.
- 560 14. Tobita M, Uysal AC, Ogawa R, Hyakusoku H, Mizuno H. Periodontal tissue
561 regeneration with adipose-derived stem cells. *Tissue Eng Part A.* 2008;14:945-53.
- 562 15. Yamada Y, Ueda M, Naiki T, Takahashi M, Hata KI, Nagasaka T. Autogenous
563 injectable bone for regeneration with mesenchymal stem cells and platelet-rich
564 plasma: Tissue-engineered bone regeneration. *Tissue Eng.* 2004;10:955-64.
- 565 16. Nakamura Y, Wang XH, Xu CS, Asakura A, Yoshiyama M, From AHL, et al.
566 Xenotransplantation of long-term-cultured swine bone marrow-derived
567 mesenchymal stem cells. *Stem Cells.* 2007;25:612-20.
- 568 17. Ide C, Nakai Y, Nakano N, Seo TB, Yamada Y, Endo K, et al. Bone marrow

- 569 stromal cell transplantation for treatment of sub-acute spinal cord injury in the rat.
570 Brain Res. 2010;1332:32-47.
- 571 18. Barcelos LS, Duplaa C, Krankel N, Graiani G, Invernici G, Katare R, et al. Human
572 CD133(+) Progenitor Cells Promote the Healing of Diabetic Ischemic Ulcers by
573 Paracrine Stimulation of Angiogenesis and Activation of Wnt Signaling. Circ Res.
574 2009;104:1095-U199.
- 575 19. Cai LY, Johnstone BH, Cook TG, Tan J, Fishbein MC, Chen PS, et al. IFATS
576 Collection: Human Adipose Tissue-Derived Stem Cells Induce Angiogenesis and
577 Nerve Sprouting Following Myocardial Infarction, in Conjunction with Potent
578 Preservation of Cardiac Function. Stem Cells. 2009;27:230-7.
- 579 20. Perin EC, Silva GV. Autologous Cell-Based Therapy for Ischemic Heart Disease:
580 Clinical Evidence, Proposed Mechanisms of Action, and Current Limitations.
581 Catheter Cardiovasc Interv. 2009;73:281-8.
- 582 21. Yoon BS, Moon JH, Jun EK, Kim J, Maeng I, Kim JS, et al. Secretory Profiles and
583 Wound Healing Effects of Human Amniotic Fluid-Derived Mesenchymal Stem
584 Cells. Stem Cells Dev. 2010;19:887-902.
- 585 22. Di Santo S, Yang ZJ, von Ballmoos MW, Voelzmann J, Diehm N, Baumgartner I, et
586 al. Novel Cell-Free Strategy for Therapeutic Angiogenesis: In Vitro Generated
587 Conditioned Medium Can Replace Progenitor Cell Transplantation. PLoS One.
588 2009;4:11.
- 589 23. Wislet-Gendebien S, Poulet C, Neirinckx V, Hennuy B, Swingland JT, Laudet E, et
590 al. In Vivo Tumorigenesis Was Observed after Injection of In Vitro Expanded
591 Neural Crest Stem Cells Isolated from Adult Bone Marrow. PLoS One. 2012;7:13.
- 592 24. Osugi M, Katagiri W, Yoshimi R, Inukai T, Hibi H, Ueda M. Conditioned Media

- 593 from Mesenchymal Stem Cells Enhanced Bone Regeneration in Rat Calvarial Bone
594 Defects. *Tissue Eng Part A*. 2012;18:1479-89.
- 595 25. Katagiri W, Osugi M, Kawai T, Ueda M. Novel Cell-Free Regeneration of Bone
596 Using Stem Cell-Derived Growth Factors. *Int J Oral Maxillofac Implants*.
597 2013;28:1009-16.
- 598 26. Carmeliet P. Angiogenesis in health and disease. *Nat Med*. 2003;9:653-60.
- 599 27. Azizi SA, Stokes D, Augelli BJ, DiGirolamo C, Prockop DJ. Engraftment and
600 migration of human bone marrow stromal cells implanted in the brains of albino rats
601 - similarities to astrocyte grafts. *Proc Natl Acad Sci U S A*. 1998;95:3908-13.
- 602 28. Bishop ET, Bell GT, Bloor S, Broom IJ, Hendry NF, Wheatley DN. An in vitro
603 model of angiogenesis: basic features. *Angiogenesis*. 1999;3:335-44.
- 604 29. Heid CA, Stevens J, Livak KJ, Williams PM. Real time quantitative PCR. *Genome*
605 *Res*. 1996;6:986-94.
- 606 30. Kawamoto T. Use of a new adhesive film for the preparation of multi-purpose
607 fresh-frozen sections from hard tissues, whole-animals, insects and plants. *Arch*
608 *Histol Cytol*. 2003;66:123-43.
- 609 31. Seo BM, Miura M, Gronthos S, Bartold PM, Batouli S, Brahim J, et al. Investigation
610 of multipotent postnatal stem cells from human periodontal ligament. *Lancet*.
611 2004;364:149-55.
- 612 32. Shirakata Y, Takeuchi N, Yoshimoto T, Taniyama K, Noguchi K. Effects of Enamel
613 Matrix Derivative and Basic Fibroblast Growth Factor with beta-Tricalcium
614 Phosphate on Periodontal Regeneration in One-Wall Intrabony Defects: An
615 Experimental Study in Dogs. *Int J Periodontics Restorative Dent*. 2013;33:641-U99.
- 616 33. Kawasaki K, Aihara M, Honmo J, Sakurai S, Fujimaki Y, Sakamoto K, et al. Effects

617 of recombinant human bone morphogenetic protein-2 on differentiation of cells
618 isolated from human bone, muscle, and skin. *Bone*. 1998;23:223-31.

619 34. Perri B, Cooper M, Laurysen C, Anand N. Adverse swelling associated with use of
620 rh-BMP-2 in anterior cervical discectomy and fusion: a case study. *Spine J*.
621 2007;7:235-9.

622 35. Patel ZS, Young S, Tabata Y, Jansen JA, Wong MEK, Mikos AG. Dual delivery of
623 an angiogenic and an osteogenic growth factor for bone regeneration in a critical
624 size defect model. *Bone*. 2008;43:931-40.

625 36. Javazon EH, Beggs KJ, Flake AW. Mesenchymal stem cells: Paradoxes of
626 passaging. *Experimental Hematology*. 2004;32:414-25.

627 37. Spencer EM, Liu CC, Si ECC, Howard GA. In vivo actions of insulin-like growth
628 factor-I (IGF-I) on bone formation and resorption in rats. *Bone*. 1991;12:21-6.

629 38. Li Y, Yu X, Lin S, Li X, Zhang S, Song YH. Insulin-like growth factor 1 enhances
630 the migratory capacity of mesenchymal stem cells. *Biochem Biophys Res Commun*.
631 2007;356:780-4.

632 39. Han XZ, Amar S. Role of insulin-like growth factor-1 signaling in dental fibroblast
633 apoptosis. *J Periodontol*. 2003;74:1176-82.

634 40. Kaigler D, Krebsbach PH, West ER, Horger K, Huang YC, Mooney DJ. Endothelial
635 cell modulation of bone marrow stromal cell osteogenic potential. *FASEB J*.
636 2005;19:665-+.

637 41. Janssens K, ten Dijke P, Janssens S, Van Hul W. Transforming growth factor-beta 1
638 to the bone. *Endocr Rev*. 2005;26:743-74.

639 42. Davis S, Aldrich TH, Jones PF, Acheson A, Compton DL, Jain V, et al. Isolation of
640 Angiopoietin-1, a ligand for the TIE2 receptor, by secretion-trap expression cloning.

641 Cell. 1996;87:1161-9.

642 43. Witzenbichler B, Maisonpierre PC, Jones P, Yancopoulos GD, Isner JM.
643 Chemotactic properties of angiopoietin-1 and -2, ligands for the endothelial-specific
644 receptor tyrosine kinase Tie2. J Biol Chem. 1998;273:18514-21.

645 44. Maisonpierre PC, Suri C, Jones PF, Bartunkova S, Wiegand S, Radziejewski C, et al.
646 Angiopoietin-2, a natural antagonist for Tie2 that disrupts in vivo angiogenesis.
647 Science. 1997;277:55-60.

648 45. Karamysheva AF. Mechanisms of angiogenesis. Biochemistry (Mosc).
649 2008;73:751-62.

650 46. Van Belle E, Witzenbichler B, Chen DH, Silver M, Chang L, Schwall R, et al.
651 Potentiated angiogenic effect of scatter factor/hepatocyte growth factor via
652 induction of vascular endothelial growth factor - The case for paracrine
653 amplification of angiogenesis. Circulation. 1998;97:381-90.

654 47. Xin XH, Yang SY, Ingle G, Zlot C, Rangell L, Kowalski J, et al. Hepatocyte growth
655 factor enhances vascular endothelial growth factor-induced angiogenesis in vitro
656 and in vivo. Am J Pathol. 2001;158:1111-20.

657 48. Corselli M, Chen CW, Crisan M, Lazzari L, Peault B. Perivascular Ancestors of
658 Adult Multipotent Stem Cells. Arterioscler Thromb Vasc Biol. 2010;30:1104-9.

659 49. Crisan M, Yap S, Casteilla L, Chen CW, Corselli M, Park TS, et al. A perivascular
660 origin for mesenchymal stem cells in multiple human organs. Cell Stem Cell.
661 2008;3:301-13.

662 50. Al-Khaldi A, Al-Sabti H, Galipeau J, Lachapelle K. Therapeutic angiogenesis using
663 autologous bone marrow stromal cells: Improved blood flow in a chronic limb
664 ischemia model. Ann Thorac Surg. 2003;75:204-9.

665 **Figure Legends**

666

667 Figure 1. MSC-CM promoted migration and proliferation of rMSCs and rPDLCs in the
668 wound-healing assay.

669

670 (A) Migration of rMSCs. Wounds were generated as described in “Materials and
671 Methods” (scale bar: 500 μm).

672 (B) The level of cellular fill within the wound area in response to MSC-CM was
673 compared with the wound-fill response in the presence of 30% FBS or serum-free
674 DMEM as control after 48 h. The migration of rMSCs and rPDLCs cultured in
675 MSC-CM was enhanced compared with rMSCs and rPDLCs cultured in DMEM
676 (-). ($n = 5$ for each group) Data are presented as means \pm SD. ** $p < 0.01$.

677

678 Figure 2. MSC-CM promoted tube formation of HUVECs.

679

680 (A) Tube formation of HUVECs was compared in BM, and in BM with MSC-CM,
681 VEGF (10 ng/mL), and MSC-CM plus anti-VEGF (10 $\mu\text{g/mL}$). After 11 days,
682 developing new blood vessels were observed under a microscope and photographed.
683 BM with MSC-CM or VEGF (10 ng/mL) stimulated tube formation (scale bar: 500
684 μm).

685 (B) The total length of blood vessels was analyzed using angiogenesis-measuring
686 software. There were statistically significant differences between the length of blood
687 vessels in the MSC-CM group and that in the other groups. ($n = 10$ for each group)
688 Data are presented as means \pm SD. * $p < 0.05$; ** $p < 0.01$.

689

690 Figure 3. MSC-CM enhanced osteogenic and angiogenic marker gene expression.

691

692 The mRNA levels of (A) *Alkaline phosphatase (ALP)*, (B) *Osteocalcin (OCN)*, (C)
693 *Runx2*, (D) *VEGF-A*, (E) *angiopoietin 1 (ANG-1)*, and (F) *angiopoietin 2 (ANG-2)*
694 genes in rMSCs cultured in MSC-CM or DMEM-10% FBS (EM; Expansion medium)
695 were assayed by real-time RT-PCR. Cells underwent lysis for extraction of total RNA
696 on day 7 of culture in MSC-CM or EM, and equal amounts of total RNA (50 ng) were
697 analyzed. The mRNA expression levels of *ALP*, *OCN*, *Runx2*, *VEGF-A*, *ANG-1*, and
698 *ANG-2* were determined relative to the level of *Glyceraldehyde 3-phosphate*
699 *dehydrogenase (GAPDH)* mRNA in each sample and were quantified by calculation
700 based on their standard curves as described in “Materials and Methods”. For
701 quantitative comparison of the levels of gene expression of the different samples, we
702 calculated the expression coefficient for each mRNA on the ordinate by dividing the
703 absolute level of expression of each mRNA (*ALP*, *OCN*, *Runx2*, *VEGF-A*, *ANG-1*, and
704 *ANG-2*) with the absolute level of expression of *GAPDH* mRNA in each sample. Each
705 point represents the mean value calculated from five independent replicates in which the
706 difference was <10%. An asterisk indicates a significant difference between the EM and
707 MSC-CM groups for the indicated gene. Data are presented as means \pm SD; $n = 5$. * p
708 < 0.05; ** p < 0.01.

709

710 Figure 4. Hematoxylin and eosin-stained histological cross-section of the periodontal
711 tissue defects 2 weeks after implantation.

712

713 (A) The defects in the MSC-CM group show a small amount of alveolar bone
714 regeneration (scale bar: 200 μ m). (B) High magnification of the defects in the MSC-CM
715 group reveals that the columnar cells were found on the surface of the regenerated
716 bone (scale bar: 50 μ m). (C, E) No alveolar bone regeneration was found in the PBS and
717 Defect groups (scale bar: 200 μ m). (D) High magnification of the defects in the PBS
718 group. (F) High magnification of the defects in the Defect group show the presence of
719 inflammatory cellular infiltration (scale bar: 100 μ m). *alveolar bone, **dental root,
720 ***regenerated bone

721

722 Figure 5. Hematoxylin and eosin-stained histological cross-section of the periodontal
723 tissue defects 4 weeks after implantation.

724

725 (A) In the MSC-CM group, a cementum-like structure and the alveolar bone with
726 alveolar crista had regenerated (scale bar: 200 μ m). (B) High magnification of the
727 defects in the MSC-CM group showed a periodontal-ligament-like structure located
728 perpendicularly between the cementum-like structure (arrow) and the alveolar bone
729 (scale bar: 100 μ m). (C) Alveolar bone regeneration was observed at a lower level in the
730 PBS group (scale bar: 200 μ m). (D) A periodontal ligament-like structure was not seen
731 between the alveolar bone and the dentin surface in the PBS group (scale bar: 100 μ m).
732 (E) Little bone regeneration in the Defect group. In addition, the volume of the gingival
733 was relatively decreased (scale bar: 200 μ m). (F) In the Defect group, dense collagen
734 fibers and granulation tissue occupied the space between the dentin surface and the
735 alveolar bone (scale bar: 100 μ m). *alveolar bone, **dental root, ***regenerated bone

736

737 Figure 6. Immunohistochemical analysis of periodontal tissue defects 2 weeks after
738 implantation.

739

740 Two weeks after implantation into the periodontal defects, tissue specimens were
741 analyzed using immunohistostaining for: CD31 (RED), a marker for rat endothelial
742 cells; CD105 (GREEN), a marker for rat stem cells; and FLK-1 (RED), a marker for
743 VEGF-R2. Cell nuclei were labeled with DAPI (blue) (scale bar: 200 μm). *alveolar
744 bone, **dental root

745 Table1. Primer and Probe Sequences Used in the Real-Time Polymerase Chain
 746 Reaction

| Gene | | Sequence | Accession No. |
|---------------|---------|---------------------------------|---------------|
| <i>ALP</i> | (F) | GACAGTCATTGAATACAAAAC | NM_053356 |
| | (R) | ACGGAATTCTTGGTTAGTA | |
| | (probe) | TAAGCCATCTCGCCTGCCAT | |
| <i>OCN</i> | (F) | GACTCTGAGTCTGACAAA | NM_013414 |
| | (R) | AGTCCATTGTTGAGGTAG | |
| | (probe) | CGGAGTCTATTCACCACCTTACTG C | |
| <i>Runx2</i> | (F) | CCTCTTATCTGAGCCAGA | NM_053470 |
| | (R) | GCAGTGTCATCATCTGAA | |
| | (probe) | CATCCATCCATTCCACCACGC | |
| <i>VEGF-A</i> | (F) | ATCCCGGTTTAAATCCTG | NM_031836 |
| | (R) | GGAACATTTACACGTCTG | |
| | (probe) | CACTGTGAGCCTTGTTCAGAGC | |
| <i>ANG1</i> | (F) | GAAGGAGGAGAAAGAAAAC | NM_053546 |
| | (R) | TCTGCTAAGTTGCTTCTC | |
| | (probe) | TGGTTACTCGTCAGACATTCATCA TCC | |
| <i>ANG2</i> | (F) | CTCTGTATGAGCACTTCTA | NM_134454 |
| | (R) | GATGCTACTGATTTTGCC | |
| | (probe) | CGGCGAGGAGTCCA ACTACA | |
| <i>GAPDH</i> | (F) | GTTCCAGTATGACTCTACC | NM_017008 |
| | (R) | TCACCCATTTGATGTTA | |
| | (probe) | TTCAACGGCACAGTCAAGGC | |

747 *ALP*, Alkaline phosphatase; *OCN* Osteocalcin; *ANG-1*, angiotensin 1; *ANG-2*,
 748 angiotensin 2.

749

750

751

752

753

754

755

756 Table2. The Levels of Cytokines Present in MSC-CM

757

| Factors | Concentration (pg/mL) |
|---------|-----------------------|
| IGF-1 | 1515.6±211.83 |
| VEGF | 465.84±108.81 760 |
| TGF-β1 | 339.82±14.41 |
| HGF | 20.32±7.89 762 |
| PDGF-BB | N.D |
| BMP-2 | N.D 764 |
| FGF-2 | N.D |
| SDF-1 | N.D 766 |

767 BMP-2, bone morphogenetic protein-2; IGF-1, insulin-like growth factor-1; VEGF,
 768 vascular endothelial growth factor; TGF-β1, transforming growth factor-β1; HGF,
 769 hepatocyte growth factor ; PDGF, plateletderived growth factor; FGF, fibroblast growth
 770 factor; SDF-1, stromalcell-derived factor-1; ND, not detected.

771

772

773

774

775

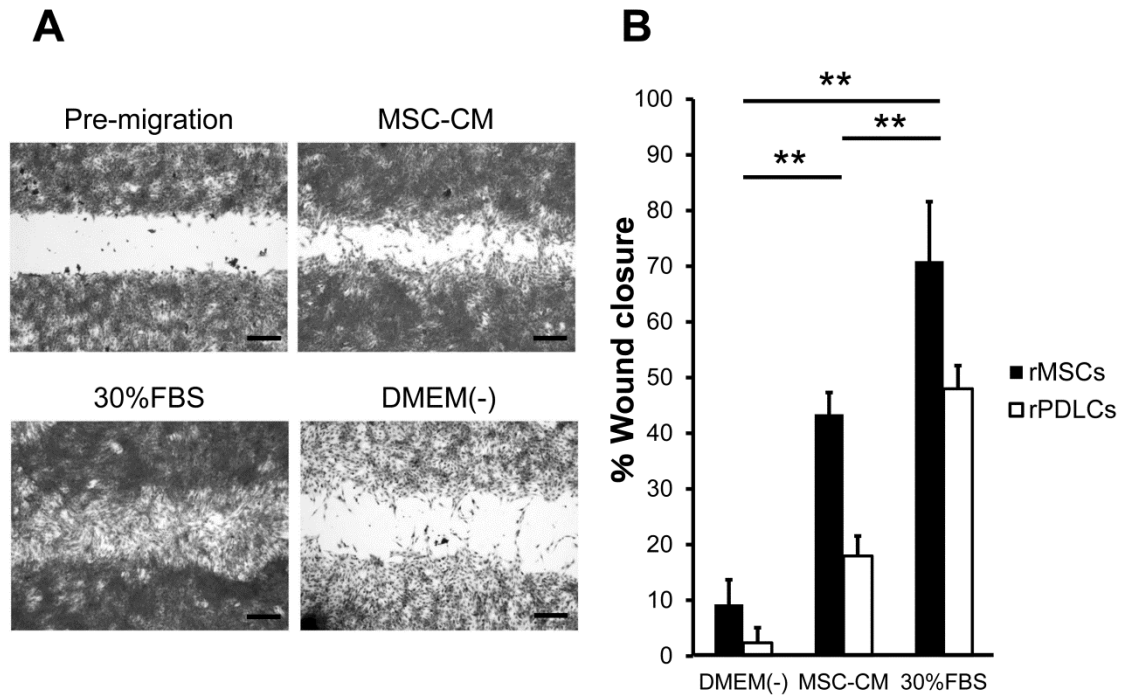
776

777

778

779

780



782

783

784

785

786

787

788

789

790

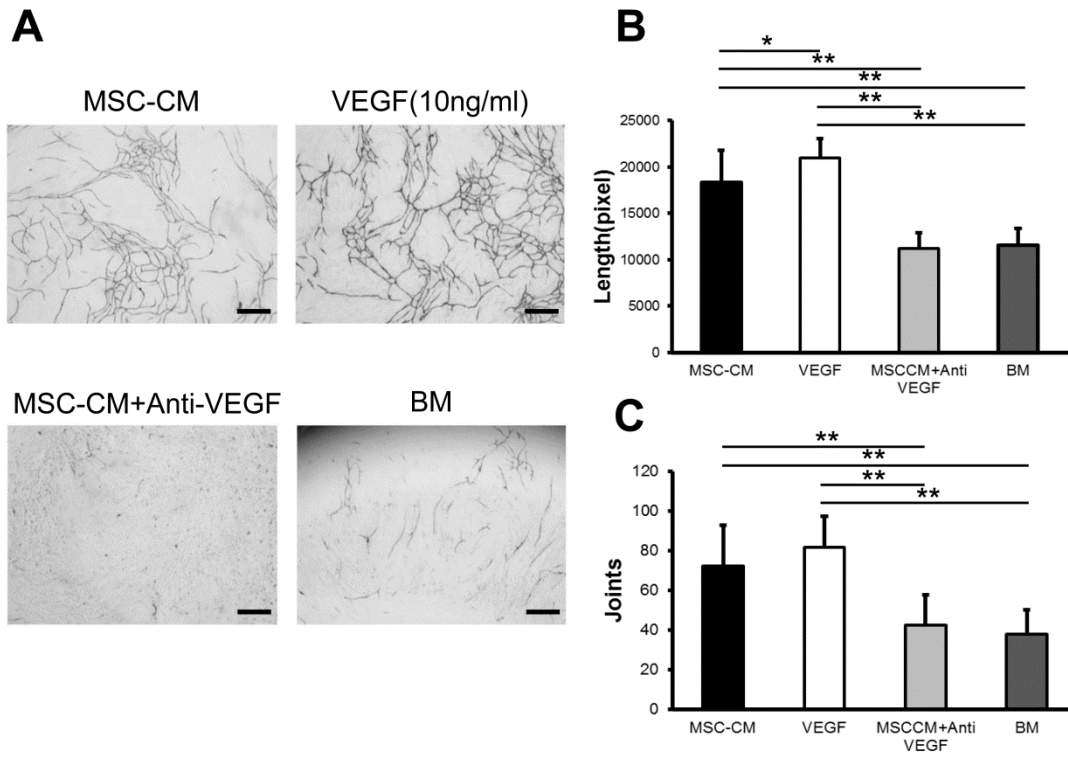
791

792

793

794

795 Fig2



796

797

798

799

800

801

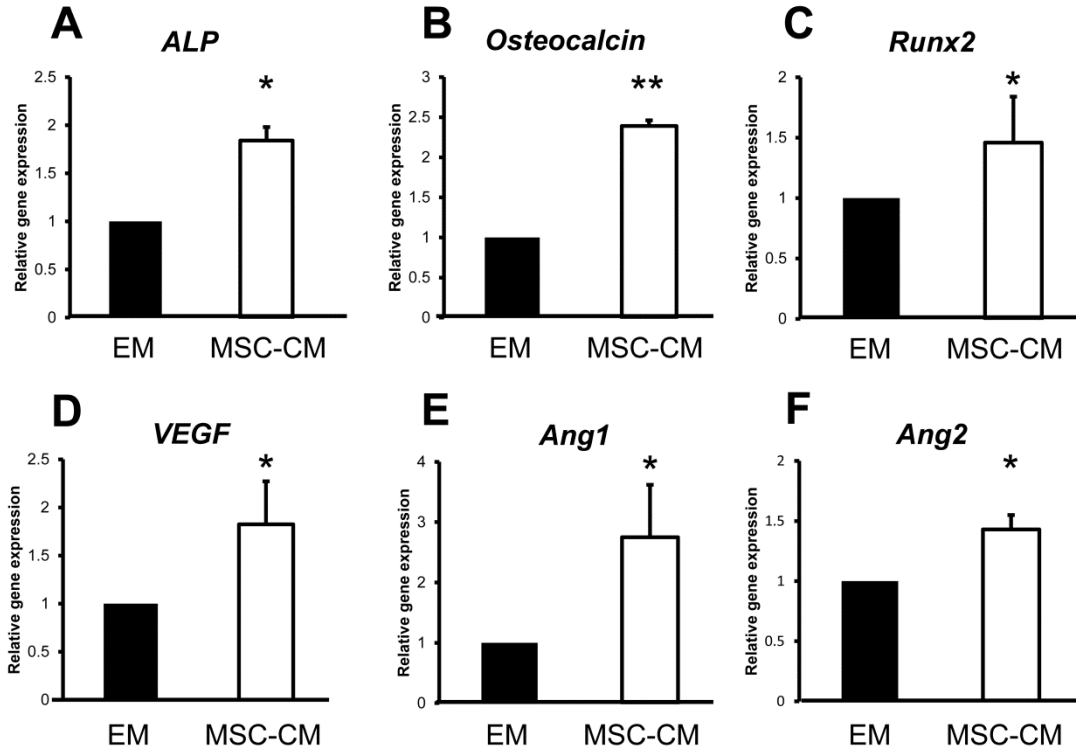
802

803

804

805

806



808

809

810

811

812

813

814

815

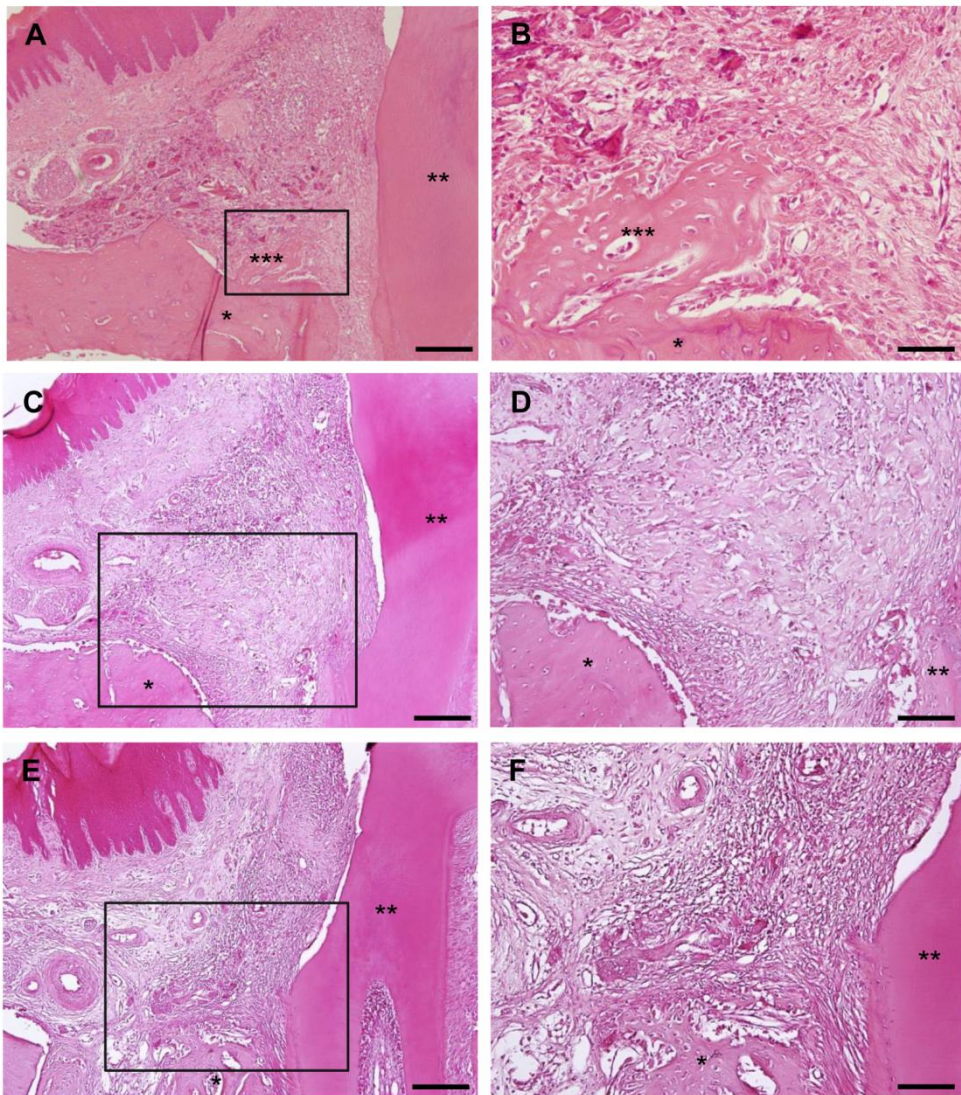
816

817

818

819

820 Fig4



821

822

823

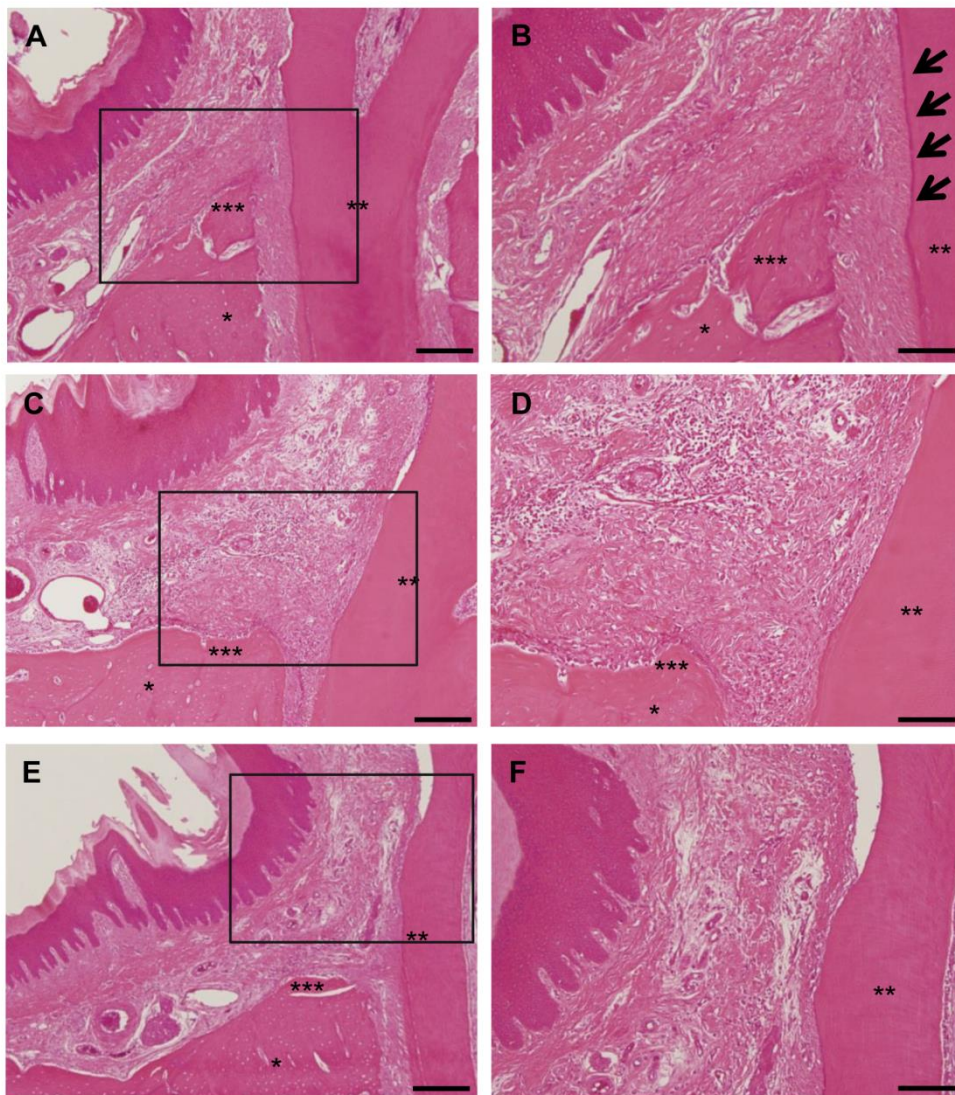
824

825

826

827

828



830

831

832

833

834

835

836

837

